

Remote video monitoring for offshore sea farms: Reliability and availability evaluation and image quality assessment via laboratory tests

David Baldo¹, Gabriele Di Renzone¹, Ada Fort¹, Marco Mugnaini¹, Giacomo Peruzzi¹, Alessandro Pozzebon², Valerio Vignoli¹

¹ Department of Information Engineering and Mathematics, University of Siena, Via Roma 56, 53100 Siena, Italy

² Department of Information Engineering, University of Padova, Via Gradenigo 6/b, 35131 Padova, Italy

ABSTRACT

In this article, the availability and reliability of a remote video monitoring system for offshore sea farming plants are studied and tested in laboratory. The scope of the system is to ensure a video surveillance infrastructure so to supervise breeding cages along with the fish inside them, in order to contrast undesired phenomena like fish poaching as well as cages damages. The system is installed on a cage floating structure: it is mainly composed of an IP camera that is controlled by a Raspberry Pi Zero which is the core of the system. Images are streamed thanks to a 3G/4G dongle, while the overall system is powered via two photovoltaic panels charging a backup battery. Simulations are carried out considering two seasonal functioning periods (i.e., winter and summer): each of them is characterised by temperature trends defined according to the average temperatures of the system deployment site, 8 km offshore the city of Piombino, Italy. In order to optimise power consumption without hindering application scenario requirements, the system operates according to a duty cycle of 2 minutes out of 15 (i.e., 8 minutes of operation per hour). The performances of the system are then tested in laboratory exploiting a climatic chamber so to simulate different environmental conditions: variations on image quality are then analysed in order to identify possible dependencies on critical situations related to specific temperature and relative humidity values and to the presence of salt in the air.

Section: RESEARCH PAPER

Keywords: Video monitoring; offshore; reliability; image quality; climatic chamber

Citation: David Baldo, Gabriele Di Renzone, Ada Fort, Marco Mugnaini, Giacomo Peruzzi, Alessandro Pozzebon, Valerio Vignoli, Remote video monitoring for offshore sea farms: Reliability and availability evaluation and image quality assessment via laboratory tests, Acta IMEKO, vol. 10, no. 4, article 7, December 2021, identifier: IMEKO-ACTA-10 (2021)-04-07

Section Editor: Silvio Del Pizzo, University of Naples 'Parthenope', Italy

Received June 1, 2021; **In final form** December 6, 2021; **Published** December 2021

Copyright: This is an open-access article distributed under the terms of the Creative Commons Attribution 3.0 License, which permits unrestricted use, distribution, and reproduction in any medium, provided the original author and source are credited.

Funding: This research was funded by Regione Toscana, project *SeaFactory*, POR FESR 2014–2020 BANDO N.2: PROGETTI STRATEGICI DI RICERCA E SVILUPPO DELLE MPMI.

Corresponding author: Alessandro Pozzebon, e-mail: alessandro.pozzebon@unipd.it

1. INTRODUCTION

Fish farming has undergone a massive growth for years now, mainly owing to various causes. Primarily, bred seafood could take part within the fight against world hunger without entailing an increase in costs, thus proving to be a cheap and valuable alternative for global food supply. Furthermore, bred seafood quality may be easily certified since the complete fish lifetime can be promptly traced throughout the breeding cycle. The upcoming affluence of this sector is also validated by some studies: a prediction on worldwide fishing market in 2030 [1]

foresees that 62 % of fish for human consumption will be produced via aquaculture by that year. In addition, the Food and Agriculture Organization (FAO) foretold a hopeful situation presuming an aquaculture production expansion up to 58% by 2022 [2]. Concerning Europe, a future discord among fish demand and supply was guessed [3], therefore fostering fish farming may turn to be an advisable initiative. Finally, in Italy aquaculture includes more than 800 companies, and most of them are situated in the Mediterranean Sea, where more than 5000 plants are located.

Offshore sea farms need to rely on surveillance systems so to contrast undesired phenomena like fish poaching as well as breeding cages damages. Therefore, in this paper an autonomous remote video monitoring system for offshore sea farms is presented along with simulations and laboratory tests whose outcomes are exploited to study its availability and reliability along with assessing performance variations and its overall effectiveness. The system is designed so to include off-the-shelf components, and in order to be energy efficient since it is powered via an energy harvesting system (i.e., two photovoltaic panels and a backup battery). Eventually, the system is installed on a cage floating structure.

Since environmental conditions may severely affect the reliability of the system in terms of quality of the acquired images, tests are performed exploiting a climatic chamber, thus allowing to simulate different environmental conditions in terms of temperature and humidity. System behaviour in extremely high and low temperatures as well as high humidity levels was tested, analysing the possible degradation in images: in particular, the environmental parameters for the various tests were identified considering the meteorological conditions of the final deployment site, as well as the ones of any general marine site in the Temperate Climate zone.

This paper is an extension of [4] and it is drawn up as follows. Some related works are reported in Section 2, while Section 3 shows the video monitoring system architecture. The reliability configurations on which simulations are carried out are outlined in Section 4, and simulations results are presented in Section 5. Section 6 is devoted to the description of the laboratory tests setup, while in Section 7 the tests results are presented and discussed. Eventually, Section 8 points out remarks and conclusions.

2. RELATED WORKS

Autonomous systems for the monitoring of fish behaviour within offshore sea farms during feeding phases was reviewed in [5]: amid sundry enabling technologies and processing techniques, the use of video recordings thorough ad-hoc systems and cameras were pointed out, thus showing their feasibility.

Video monitoring systems that are deployed in marine contexts are mainly designed for coastal safeguard so to assess erosion [6]-[9] rather than for sea farms surveillance. Such systems make use either of standard IP cameras [6], [7], like the one within the system presented in this paper, or of embedded cameras directly controlled by a single-board computer as Raspberry Pi [8], which is the control unit of the system that will be presented in the following Section. Similarly, remote video monitoring systems may be also exploited to assess post-storm recoveries within beaches. To this end, in [9] such a system is developed and tested in Australia. Therein, a video monitoring framework was employed for the assessment of erosion levels of sandy coastlines that experienced severe storms. At the same time, such facility was used as well to evaluate the recovery level after storms, highlighting adequate system reliability and effectiveness. Nonetheless, these sorts of monitoring infrastructures are usually ashore installed thus easing, for instance, data transmission (which can be accomplished without resorting to wireless solutions) and system maintenance. However, the literature also comprehends works implementing video monitoring systems that are installed on offshore buoys within breeding plants: in [10], cameras are set up within the fish cages, while video streaming is ensured by a radio frequency

system that is installed on board of the buoy. Similarly, works reported in [11], [12] extend such a surveillance system. For what concerns the application scenario, [13] shares a similar context with respect to the one of this paper, since the authors propose a remote monitoring system for offshore oceanic sea farms made of floating cages. The system includes cameras, sonars, and telemetry devices, and it is installed on cage feed buoys (which are like the one that will be introduced later on). Unfortunately, though, images are not ashore streamed because they are recorded and stored on board of a boat. On the other hand, marine video monitoring systems are additionally devised so to operate underwater, fulfill submarine investigation and exploration purposes [14], as well as for proper aquaculture ponds characterised by turbid water [15].

Concerning video monitoring systems in a broad sense (i.e., which are employed in diverse contexts with respect to the marine one) that rely on photovoltaic energy harvesting systems and a backup battery, works within [16], [17] confirm the suitability of such a technique thus underlining the potential effectiveness of the solution proposed in this paper.

Image quality may be judged by means of several metrics so to measure the grade of similarity between two pictures. Indeed, cameras capabilities can be objectively evaluated by resorting to the aforesaid metrics. This paper makes use of a well-known technique, that will be introduced later, which received a wide approval in the academic world. However, and for the sake of completeness, some newer approaches are also cited below so to provide readers with additional references. For instance, in [18] image quality assessment is performed from a vectorial perspective by making recourse to the vector root mean squared error which allows for an alternative to the biggest limitations (e.g., noise cancellation or detail preservation) of mean-squared-error-based techniques. On the other hand, image quality assessment may be also accomplished by means of machine learning techniques, and in particular [19] tackles the problem by falling back on deep neural networks. They can capture high-order statistics of image feature descriptors and storing them into a dictionary thus turning out into a deep dictionary encoding network. Finally, captured images from remote video monitoring systems may suffer from artifacts stemming from equipment wear as well as from bad weather. In order to enhance image quality, it is favourable setting up methods aiming at mitigating such shortcomings. Therefore, in [20] a solution to the problem is proposed by establishing an algorithm for dehazing images which can be applied to a myriad of contexts, especially the harsher ones like offshore.

3. SYSTEM ARCHITECTURE

The block diagram of the video monitoring system is depicted in Figure 1, and it is composed of 3 main building blocks (i.e., power supply, control and communications and camera).

The power supply block contains 2 photovoltaic panels providing 20 W each, whose task is either to power up the whole system and to recharge a 12 V, 25 Ah lead-acid backup battery through a solar charge controller. The power supply block is only composed of off-the-shelf components: such a decision was made so to develop the prototype as soon as possible to test its effectiveness. The core of the power supply system is the solar charge controller. It is responsible for correctly powering up the control and communications block and the camera in function of both the battery charge level and the power coming from the photovoltaic panels. Indeed, whenever they are exposed to

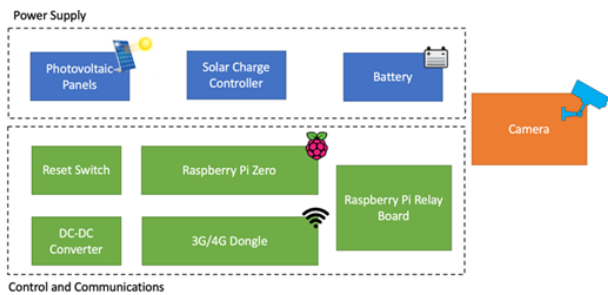


Figure 1. Video monitoring system block scheme.

enough sunlight, the solar charge controller manages the harvested energy for running the whole system as well as for recharging the backup battery. On the contrary, whenever the harvested energy is scant (e.g., during the night), the solar charge controller draws energy from the battery so to supply the system. Photovoltaic panels are fundamental for the long-term functioning of the system. Indeed, such a prototype is offshore installed, and it is supposed to operate for at least a 6-month timespan, while the mere backup battery only ensures a 48-hour autonomy. Thus, additionally highlights the low-power feature of the system components (that will be introduced below) along with the effectiveness of the duty-cycling functioning policy (that will be addressed in the next Section). However, a complete battery discharge is extremely unlikely since it would be the consequence of several hours of darkness.

The control and communications block is the core of the system since it manages the duty cycling of the camera along with images capturing and transmitting towards a remote server, while minimizing power consumption by the activation of the inner elements only for the minimum amount of time needed. Such a working flow is obtained by the following off-the-shelf components:

- DC-DC converter which filters out the power supply coming from the appropriate building block so to correctly power each of the system elements;
- Raspberry Pi Zero is the control unit of the system due to Python scripts managing both the camera and the duty cycling of all of the other components;
- Raspberry Pi relays board contains relay switches that are directly controlled by the Raspberry Pi so to turn on and off the camera and the other system elements whenever they are needed and only for the strictly necessary time in order to limit the overall power consumption;
- 3G/4G dongle provides Internet connectivity that is exploited to send the captured images and the debug logs to a remote server in order to perform diagnostic;
- Reset switch performs a daily hardware reset of the whole system acting as a sort of long-term watchdog timer so to overcome software issues or unexpected behaviours.

The camera is an off-the-shelf outdoor IP one produced by Hikvision, which is especially designed so to resist to marine environments.

All the elements composing the control and communications block are housed within an IP56 box, while the complete system is mounted on a support pole (see Figure 2) which is offshore installed on a breeding cage floating structure (see Figure 3).

4. RELIABILITY CONFIGURATIONS

The application scenario for this video monitoring system does not necessitate of real-time image streaming. In particular,



Figure 2. Realization of the video monitoring system: photovoltaic panels (left) and pole with camera and IP56 box containing the electronics (right).

only snapshots on a regular basis (i.e., one every 15 minutes) are required. Therefore, in order to meet functioning requirements, the system operates for a time span of 2 minutes every quarter of an hour within which the picture is taken and remotely sent via the Internet. In so doing, only 8 minutes per hour of system activity is experienced (i.e., 172 minutes per day), thus also optimizing power consumption.

For what concerns weather conditions the system is exposed, two seasonal functioning periods are identified on which availability and reliability simulations are carried out:

- **Winter**, that is made up of 3 8-hour time slots, that are daily repeated, which are in turn characterised by a temperature of 5°C, 10°C and 15°C;
- **Summer**, which accounts for 3 8-hour time slots, which are daily repeated, that are respectively characterised by a temperature of 20°C, 25°C and 30°C.

Such temperatures are considered because of the future system deployment scenario: 8 km offshore the city of Piombino, Italy.

Simulation parameters are summarised in Figure 4, while availability and reliability simulation schemes are shown in Figure 5 [21]-[24]. The MIL HDBK 217F database was selected to evaluate individual component failure rates at different temperatures considering an environment of the kind Naval Unsheltered (NU). Unfortunately, such parameters are usually not available from component producers, therefore a conservative approach given by the mentioned database results in worst condition scenarios was followed.

5. SIMULATION RESULTS

As shown in Figure 6, simulations were performed by means of the BlockSim software (by Reliasoft) on the two scenarios previously described. In the upper picture the availability, that is the ratio between the mean time between failures and the sum of the overmentioned time plus the mean time to restoration ($MTBF/(MTBF+MTTR)$), over time (considering a restoration time of 48 hours) is shown, while in the bottom picture the reliability trend over time is represented considering as failure rates the inverses of the figures cited in Table of Figure 4. Both results prove that the summer period presents a decrease in the final time values with respect to the winter one. Such results agree with what expected by the theory connected to the exploitation of the MIL HDBK 217F database where



Figure 3. Autonomous remote video monitoring system prototype offshore installed on a cage floating structure.

temperature-based degradation, under a fixed environment, takes place. To simulate the availability model, a fixed 48 h repair time was considered. Of course, due to the very small number of electronic components and to the low system complexity, the system has to be tested especially for wintertime on long periods since the overall MTBF is considerably high at those temperatures. Moreover, both the selected duty cycle for system exploitation and the power consumption reduction limit the internal temperature raise keeping it almost constant, without significant degradation rates apparently induced on individual electronics.

Simulations do not include condensation due to temperature excursions. Therefore, the rusting due to salty environment condensation is not considered in the results. The overall system is housed within an IP56 box presenting holes to which siphons

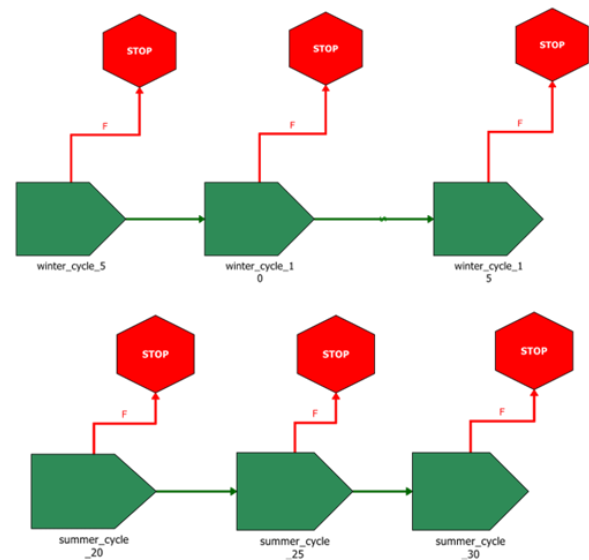


Figure 5. Availability and reliability simulation schemes: winter and summer working periods.

are connected so to allow heat dissipation via air circulation. However, this also implies that salty air enters within the box coming into contact with system components. This is far from being an optimal solution, albeit it is sufficient for the prototype. Indeed, the latter is supposed to operate just for 6 months during which damages due to saltiness should be limited. Consequently, salty air from the sea is assumed to be present around the electronics especially if maintenance activities will be performed. Hence, such environment is by far challenging for what concerns junctions and soldering rather than single component performances. In the future, in case of failure, a root cause analysis could be applied on single assets so to verify whether this hypothesis is confirmed or not. The system availability without the charging station is not taken into consideration because the system would not work enough time to gather the requested data, and thus it is excluded by the simulations.

6. EXPERIMENTAL SETUP

Following the simulations concerning the availability and reliability of the system, a set of tests was planned and performed in laboratory, with the aim of identifying possible negative effects on the acquired images due to the severe variations in terms of environmental conditions that the system, and the video camera in particular, is subject to. So to expose the system to different environmental conditions, the control and communication block, as well as the camera itself, were detached from the energy harvesting system and positioned inside a climatic chamber,

Elements	Characteristics	Model	Temperature [°C]					
			5	10	15	20	25	30
			MTBF [h]					
Solar Charge Controller	12-24 V/20 A	CMDT-A2420	94.000,00	93.000,00	92.000,00	91.000,00	85.000,00	81.000,00
Reset Switch	12 V	JK11S V1.1	1.067.577,68	1.067.577,68	1.067.577,70	1.067.577,70	1.067.577,70	1.067.577,68
Battery	12 V/25 Ah	Victron Energy AGM12-25	61.674.757,20	61.674.757,20	61.674.757,00	15.059.188,00	11.934.038,00	9.530.309,94
DC-DC Converter	-	-	65.444.336,31	5.090.737,61	5.145.730,20	4.591.034,50	4.111.841,80	3.693.087,57
Raspberry Pi	-	Zero	9.609.216,30	9.607.060,01	9.604.400,90	9.601.147,80	9.597.196,80	9.592.432,50
3G/4G Dongle	-	Huawei E3372	79.365,08	79.365,08	79.365,08	79.365,08	79.365,08	79.365,08
Raspberry Pi Relay Board	-	-	266.894,42	266.894,42	266.894,42	266.894,42	266.894,42	266.894,42
Total MBTF [h]			79.336.147,00	78.579.392,00	77.930.725,00	30.756.208,00	27.141.913,00	24.313.667,20

Figure 4. Simulation Parameters.

whose size did not allow the insertion of the complete system. Indeed, an ACS Angelantoni HYGROS 250 environmental test chamber, whose internal volume is $600 \times 535 \times 700 \text{ mm}^3$ ($W \times D \times H$), was used to perform tests. The climatic chamber is characterised by a temperature range from $-40 \text{ }^\circ\text{C}$ to $+180 \text{ }^\circ\text{C}$, and a relative humidity range from 10 % to 98 % in the temperature range from $+5 \text{ }^\circ\text{C}$ to $+95 \text{ }^\circ\text{C}$. It is important to point out that the relative humidity concentration depends on the psychrometric principle; therefore, the relative humidity value strictly depends on the temperature values. The minimum relative humidity values RH_{\min} are expressed in the following bulleted list:

- $RH_{\min} = \text{floating}$ for $T \leq 0 \text{ }^\circ\text{C}$;
- $RH_{\min} = 55\%$ for $T = +10 \text{ }^\circ\text{C}$;
- $RH_{\min} = 30\%$ for $T = +20 \text{ }^\circ\text{C}$;
- $RH_{\min} = 17\%$ for $T = +30 \text{ }^\circ\text{C}$;
- $RH_{\min} = 10\%$ for $T \geq +40 \text{ }^\circ\text{C}$;

where T is the temperature value.

Tests were performed following the subsequent approach. The climatic chamber was programmed so to simulate the maritime weather, which has a relative humidity value around 80%; therefore, it performs the following temperature and relative humidity pairs, which for the sake of simplicity are numbered from the first to the last executed test:

1. $T = -10 \text{ }^\circ\text{C}$ with $RH = \text{floating}$;
2. $T = 0 \text{ }^\circ\text{C}$ with $RH = \text{floating}$;
3. $T = +10 \text{ }^\circ\text{C}$ with $RH = 80 \%$;
4. $T = +20 \text{ }^\circ\text{C}$ with $RH = 80 \%$;
5. $T = +30 \text{ }^\circ\text{C}$ with $RH = 80 \%$;
6. $T = +40 \text{ }^\circ\text{C}$ with $RH = 80 \%$;
7. $T = +50 \text{ }^\circ\text{C}$ with $RH = 80 \%$.

The whole system was positioned inside the climatic chamber, and it was cycled for each temperature humidity pair. Moreover, 300 ml of saturated solution of salt in water was put along with the system to simulate the real conditions of the final deployment site. For the sake of completeness, it must be said that the battery and the 3G/4G dongle are exempt from the test. The first one was completely removed since lead-acid batteries are subjected to breakdown when extreme and abrupt changes of temperature values occur; thus, the system was mains powered exploiting a cable gland. The latter one, instead, was positioned outside the climatic chamber since the chassis of the HYGROS 250 is made of metal (except for the porthole), so it compromises the connection capability of the dongle. Test setup can be seen in Figure 7.

The camera was fixed to the climatic chamber so to avoid misplacements of the pictures, while tests were in progress. Since the aim of the tests was to identify possible image degradations, a frame control image, shown in Figure 8, was selected. Such image was chosen with the aim of comparing the details and chromatic differences that may occur when the camera is subjected to different environments. The control image was positioned at the porthole, inside the climatic chamber; then, a picture of the control image was taken at a temperature of $25 \text{ }^\circ\text{C}$ and a relative humidity of 50 %, with the light of the climatic chamber switched on.

The test started setting the climatic chamber as introduced in the aforesaid numbered list. As soon as the climatic chamber reached the defined temperature and relative humidity pair, the whole system was held at those levels for 10 minutes so to allow the electronics inside the climatic chamber to reach a steady state. At this point the inner light was switched on; the system was powered up, and 500 pictures were taken at a rate of approximately one picture every two seconds. Tests and related results are presented in the following Section.

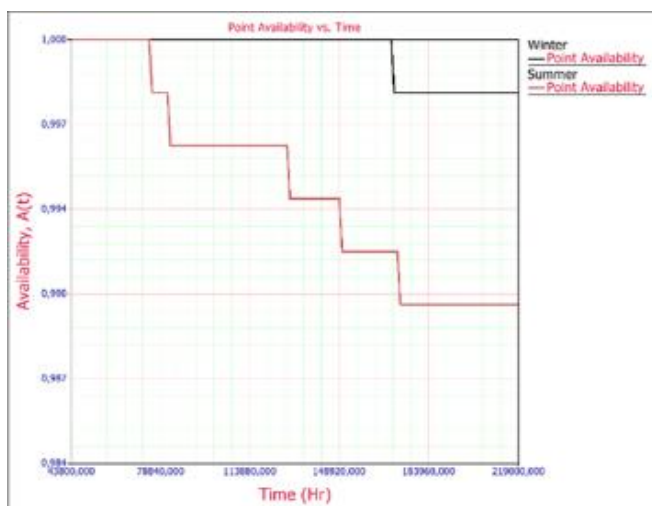


Figure 6. Availability and Reliability simulation results during winter and summer working periods.



Figure 7. Test setup: control image fixed at the porthole can be seen on the left, while the camera and the system are positioned inside the climatic chamber together with the glass containing the saturated solution of salt and water.



Figure 8. Image used for the tests.

7. TEST RESULTS AND DISCUSSION

Tests aimed at assessing the video surveillance monitoring system performances, under different environmental conditions, from the point of view of two different benchmarks: picture acquisition time and picture quality.

Acquisition times were directly sampled by the video monitoring system. Then, for each of the experimental set, those times were averaged: the relative results are reported in Figure 9. The maximum mean acquisition time (i.e., 1173 ms) was experienced at -10 °C, while the minimum one (i.e., 1126 ms) was recorded at 30 °C and 80 % of relative humidity. However, despite the mean acquisition time trend is not constant, it could be considered so since the difference amid the maximum and the minimum is just 47 ms, thus underlying the fact that no significant performances variation is present.

The assessment of the variation of picture quality was carried out by resorting to the Multiscale Structural Similarity (MS-SSIM) index for image quality [25]. This method compares two images and provides as output an index (i.e., the MS-SSIM) representing how much these pictures are similar: the closer the MS-SSIM to 1, the more similar the images. If MS-SSIM for two images is 1, then they are identical. Therefore, each of the pictures taken by the camera during the experimental sets were compared to the control one by means of the MS-SSIM, and then the resulting MS-SSIMs were averaged for each experimental set. Mean MS-SSIM trend is reported in Figure 10, while Figure 11 shows the control picture along with one picture for each of the

experimental sets. Although all the pictures seem to look the same, as the mean MS-SSIM trend shows, they slightly differ. As expected, the maximum mean MS-SSIM (i.e., 0.799) was experienced at 20 °C and 80 % of relative humidity: indeed, the control picture was taken at room temperature, therefore the most significant environmental variation was the relative humidity content. On the other hand, the minimum mean MS-SSIM (i.e., 0.685) was recorded at -10 °C. Qualitatively, the system better performed at higher temperatures, indeed meaningful discrepancy amid lower temperatures experimental sets and higher temperatures ones took place. This behaviour can be justified by the mechanical stress induced on the camera infrastructure. Electronics cannot be responsible for picture variability over temperature and humidity stress for two reasons. The first one is that the timing and temperature range of experiments are so limited that electronics are not likely to be affected. The second one is that relative humidity can affect both the optical transparency and the plastic support can be deformed in such temperature range. Therefore, it is likely that in such testing condition the plastic support holding the camera optics can be affected influencing camera acquisition and therefore the images.

8. CONCLUSIONS

The aim of this paper was to describe the architecture of an autonomous video monitoring system to be employed for the remote control of offshore breeding cages in aquaculture plants. The proposed solution is characterised by energy self-sufficiency thanks to an energy harvesting system based on the use of photovoltaic panels. In order to demonstrate the usability of the system, as a first step simulations were performed in order to validate its reliability and availability. Then, a set of tests were carried out, exploiting a climatic chamber, so to identify possible image degradations due to different environmental conditions. Results prove that the system can be successfully employed in the proposed application scenario for both winter and summer environmental settings, while degradations occurring at extreme climatic conditions are still compliant with the video monitoring purpose of the whole system. The current analysis is not including considerations on the possible rusting caused by the operation scenario either on soldering, junctions and connectors which should be included in the future in order perform an utter system reliability and availability analysis. Moreover, while the

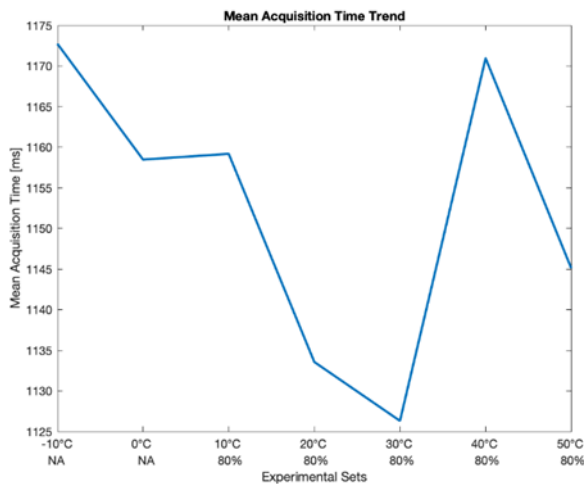


Figure 9. Mean acquisition times.

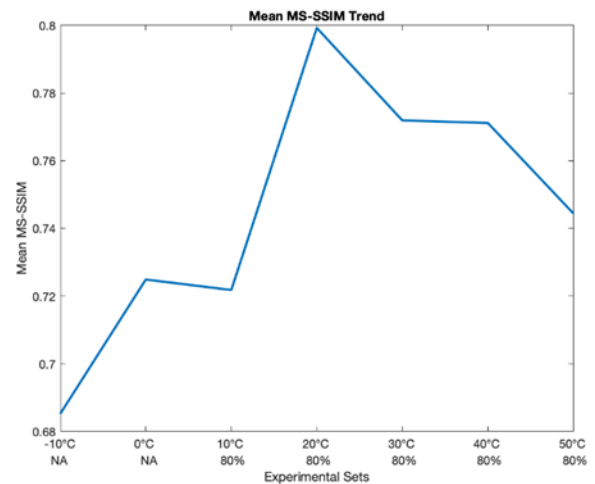


Figure 10. Mean MS-SSIM trend.

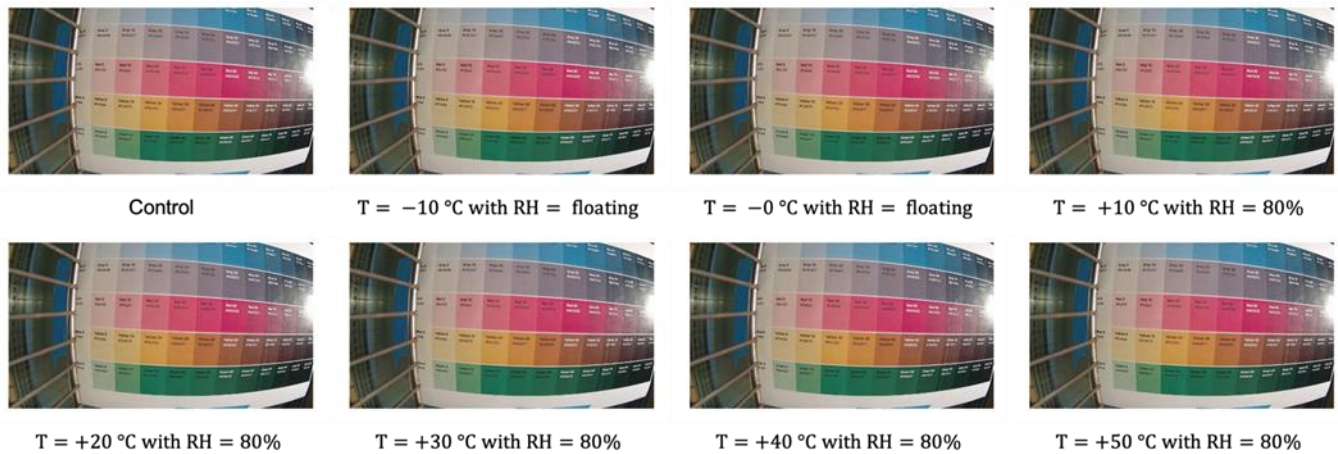


Figure 11. Examples of acquired images for each test phase.

tests demonstrated the reliability of the image acquisition procedure, a long-term field test, performed on site, is expected to be carried out in the near future in order to study the behaviour of the system in its real deployment scenario.

ACKNOWLEDGEMENT

The authors would like to thank Agroittica Toscana SRL for its support in all the field test activities and Alta Industries SRL for its support for the tests carried out in the climatic chamber.

REFERENCES

- [1] M. Kobayashi, S. Msangi, M. Batka, S. Vannuccini, M. M. Dey, J. L. Anderson, Fish to 2030: the role and opportunity for aquaculture, *Aquaculture Economics & Management* 19 (3) (2015), pp. 282-300.
DOI: [10.1080/13657305.2015.994240](https://doi.org/10.1080/13657305.2015.994240)
- [2] A. Fredheim, T. Reve, Future Prospects of Marine Aquaculture, Proceedings of OCEANS 2018 MTS/IEEE, Charleston, SC, USA, 22-25 October 2018, pp. 1-8.
DOI: [10.1109/OCEANS.2018.8604735](https://doi.org/10.1109/OCEANS.2018.8604735)
- [3] L. Angulo Aranda, P. Salamon, M. Banse, M. Van Leeuwen, Future of Aquaculture in Europe: Prospects under current conditions, Proceedings of XV EAAE Congress, "Towards Sustainable Agri-food Systems: Balancing Between Markets and Society", Parma, Italy, 29 August-1 September 2017.
- [4] D. Baldo, A. Fort, M. Mugnani, G. Peruzzi, A. Pozzebon, V. Vignoli, Reliability and Availability Evaluation of an Autonomous Remote Video Monitoring System for Offshore Sea Farms, Proceedings of 2020 IMEKO TC-19 International Workshop on Metrology for the Sea, Naples, Italy, 5-7 October 2020. Online [Accessed 10 December 2021]
<https://www.imeko.org/publications/tc19-Metrosea-2020/IMEKO-TC19-MetroSea-2020-04.pdf>
- [5] D. Li, Z. Wang, S. Wu, Z. Miao, L. Du, Y. Duan, Automatic recognition methods of fish feeding behaviour in aquaculture: A review, *Aquaculture*, 528 (15) (2020), 735508.
DOI: [10.1016/j.aquaculture.2020.735508](https://doi.org/10.1016/j.aquaculture.2020.735508)
- [6] R. Taborada, A. Silva, COSMOS: A lightweight coastal video monitoring system, *Computers & Geosciences*, 49 (2012), pp. 248-255.
DOI: [10.1016/j.cageo.2012.07.013](https://doi.org/10.1016/j.cageo.2012.07.013)
- [7] N. Valentini, A. Saponieri, L. Damiani, A new video monitoring system in support of Coastal Zone Management at Apulia Region, Italy, *Ocean & Coastal Management*, 142 (2017), pp. 122-135.
DOI: [10.1016/j.ocecoaman.2017.03.032](https://doi.org/10.1016/j.ocecoaman.2017.03.032)
- [8] R. Archetti, M.G. Gaeta, F. Addona, L. Cantelli, C. Romagnoli, F. Sisti, G. Stanghellini, Coastal vulnerability assessment through low-cost video monitoring: the case of riccione, Proceedings of SCACR 2019 - International Short Course/Conference on Applied Coastal Research, 2019.
- [9] K. D. Splinter, D. R. Strauss, R. B. Tomlinson, Assessment of post-storm recovery of beaches using video imaging techniques: A case study at Gold Coast, Australia, *IEEE Transactions on geoscience and remote sensing*, 49 (12) (2011), pp. 4704-4716.
DOI: [10.1109/TGRS.2011.2136351](https://doi.org/10.1109/TGRS.2011.2136351)
- [10] B. Fullerton, M.R. Swift, S. Boduch, O. Eroshkin, G. Rice, Design and analysis of an automated feed-buoy for submerged cages, *Aquacultural Engineering*, 32 (1) (2004), pp. 95-111.
DOI: [10.1016/j.aquaeng.2004.03.008](https://doi.org/10.1016/j.aquaeng.2004.03.008)
- [11] S.J. Boduch, J.D. Irish, Aquaculture Feed Buoy Control-Part 1: System Controller, Proceedings of OCEANS 2006, Boston, MA, USA, 18-21 September 2006.
DOI: [10.1109/OCEANS.2006.307132](https://doi.org/10.1109/OCEANS.2006.307132)
- [12] J. D. Irish, S. J. Boduch, Aquaculture feed buoy control-Part 2: Telemetry, data handling and shore-based control, Proceedings of OCEANS 2006, Boston, MA, USA, 18-21 September 2006.
DOI: [10.1109/OCEANS.2006.307133](https://doi.org/10.1109/OCEANS.2006.307133)
- [13] A. P. M. Michel, K. L. Croff, K. W. McLetchie, J. D. Irish, A remote monitoring system for open ocean aquaculture, Proceedings of OCEANS '02 MTS/IEEE, Biloxi, MI, USA, 29-31 October 2002.
DOI: [10.1109/OCEANS.2002.1192017](https://doi.org/10.1109/OCEANS.2002.1192017)
- [14] H. Wang, W. Cai, J. Yang, Q. Chen, Design of HD video surveillance system for deep-sea biological exploration, Proceedings of 2015 IEEE 16th International Conference on Communication Technology (ICCT), Hangzhou, China, 18-20 October 2015, pp. 908-911.
DOI: [10.1109/ICCT.2015.7399971](https://doi.org/10.1109/ICCT.2015.7399971)
- [15] C.C. Hung, S.C. Tsao, K.H. Huang, J.P. Jang, H.K. Chang, F.C. Dobbs, A highly sensitive underwater video system for use in turbid aquaculture ponds, *Scientific Reports*, 6 (1) (2016), pp. 1-7.
DOI: [10.1038/srep31810](https://doi.org/10.1038/srep31810)
- [16] L. Qi-An, L. Peng, F. Gui-zeng, L. Ping, L. Chang-lin, Z. Jun-xiao, The solar-powered module design of wireless video monitoring system, *Energy Procedia*, 17 (2012), pp. 1416-1424.
DOI: [10.1016/j.egypro.2012.02.261](https://doi.org/10.1016/j.egypro.2012.02.261)
- [17] K. Abas, K. Obraczka, L. Miller, Solar-powered, wireless smart camera network: An IoT solution for outdoor video monitoring, *Computer Communications*, 118 (2018), pp. 217-233
DOI: [10.1016/j.comcom.2018.01.007](https://doi.org/10.1016/j.comcom.2018.01.007)
- [18] A. De Angelis, A. Moschitta, F. Russo, P. Carbone, A vector approach for image quality assessment and some metrological considerations, *IEEE Transactions on Instrumentation and Measurement*, 58 (1) (2008), pp. 14-25.
DOI: [10.1109/TIM.2008.2004982](https://doi.org/10.1109/TIM.2008.2004982)
- [19] Q. Jiang, W. Gao, S. Wang, G. Yue, F. Shao, Y. S. Ho, S. Kwong, Blind image quality measurement by exploiting high-order

- statistics with deep dictionary encoding network, *IEEE Transactions on Instrumentation and Measurement*, 69 (10) (2020), pp. 7398-7410.
DOI: [10.1109/TIM.2020.2984928](https://doi.org/10.1109/TIM.2020.2984928)
- [20] Z. Zhu, H. Wei, G. Hu, Y. Li, G. Qi, N. Mazur, A novel fast single image dehazing algorithm based on artificial multiexposure image fusion, *IEEE Transactions on Instrumentation and Measurement*, 70 (2020), pp. 1-23.
DOI: [10.1109/TIM.2020.3024335](https://doi.org/10.1109/TIM.2020.3024335)
- [21] G. Ceschini, M. Mugnaini, A. Masi, A reliability study for a submarine compression application, *Microelectronics Reliability*, 42 (9-11) (2002), pp. 1377–1380.
DOI: [10.1016/S0026-2714\(02\)00153-1](https://doi.org/10.1016/S0026-2714(02)00153-1)
- [22] M. Catelani, L. Ciani, M. Mugnaini, V. Scarano, R. Singuaroli, Definition of safety levels and performances of safety: Applications for an electronic equipment used on rolling stock, *Proceedings of 2007 IEEE Instrumentation & Measurement Technology Conference IMTC*, Warsaw, Poland, 1-3 May 2007, 4258348.
DOI: [10.1109/IMTC.2007.379086](https://doi.org/10.1109/IMTC.2007.379086)
- [23] M. Mugnaini, M. Catelani, G. Ceschini, A. Masf, F. Nocentini, Pseudo time-variant parameters in centrifugal compressor availability studies by means of Markov models, *Microelectronics Reliability*, 42 (9-11) (2002), pp. 1373–1376.
DOI: [10.1016/S0026-2714\(02\)00152-X](https://doi.org/10.1016/S0026-2714(02)00152-X)
- [24] A. Fort, F. Bertocci, M., Mugnaini, V. Vignoli, V. Gaggi, A. Galasso, M. Pieralli, Availability modeling of a safe communication system for rolling stock applications, *Proceedings of 2013 IEEE International Instrumentation and Measurement Technology Conference (I2MTC)*, Minneapolis, MN, USA, 6-9 May 2013, pp. 427–430.
DOI: [10.1109/I2MTC.2013.6555453](https://doi.org/10.1109/I2MTC.2013.6555453)
- [25] Z. Wang, E. P. Simoncelli and A. C. Bovik, Multiscale structural similarity for image quality assessment, *Proceedings of The Thirty-Seventh Asilomar Conference on Signals, Systems & Computers*, Pacific Grove, CA, USA, 9-12 November 2003, pp. 1398-1402.
DOI: [10.1109/ACSSC.2003.1292216](https://doi.org/10.1109/ACSSC.2003.1292216)